Title
Correlation between measured path function and relative humidity

Permalink
https://escholarship.org/uc/item/79b6m3s7

Author
Boileau, Almerian R

Publication Date
1959-02-01

Visibility Laboratory
University of California
Scripps Institution of Oceanography
San Diego 52, California

CORRELATION BETWEEN MEASURED PATH FUNCTION

AND RELATIVE HUMIDITY

Almerian R. Boileau

Approved:

Approved for Distribution:

Seibert Q. Duntley, Director
Visibility Laboratory

Roger Revelle, Director
Scripps Institution of Oceanography

Correlation Between Measured Path Function

and Relative Humidity[*]

Almerian R. Boileau

Scripps Institution of Oceanography, University of California

La Jolla, California

INTRODUCTION AND SUMMARY

The Visibility Laboratory of the University of California, La Jolla Campus, is engaged in an on-going research program studying image transmission through the atmosphere. The paper "Image Transmission by the Troposphere I,"[4] published in the Journal of the Optical Society of America, discusses this program. In that paper correlation between certain optical and meteorological parameters is indicated. The study of this correlation has continued and this report describes the results of data gathered from a second formation flight of two airplanes, the instrumented B-29 and a microwave refractometer-equipped C-131 from Patrick Air Force Base squadron.

It was found that when the relative humidity is high, approximately 85 percent and higher, small changes in relative humidity are accompanied by large changes of path function, i.e., the scattering of radiant flux from particles in the air; when the relative humidity is approximately 60 percent or lower, large changes in relative humidity are accompanied by small changes of path function; and in the range of relative humidities from 65 percent to 85 percent a more complicated relationship between relative humidity and path function exists.

PROCEDURE

On 6 May 1957 the B-29 and C-131 took off from Patrick Air Force Base at approximately 1330 E.S.T. The two airplanes were taken to 18,000 feet altitude. During this ascent a record of air temperature was made. At 1436 E.S.T. at 18,000 feet, a descent was started in which the two airplanes, flying in formation, maintained a descent rate of approximately 1000 feet/minute. In the descent the B-29 was held in a level attitude (indicated by a bubble level attached to the pilot's aisle stand), with the power reduced and landing gear extended to increase drag. During the descent the temperature and the optical parameters for which the B-29 and the microwave refraction modulus for which the C-131 is instrumented was recorded in the C-131. The descent ended at 500 feet at 1509 E.S.T. The records of all parameter values are continuous as a function of altitude.

INSTRUMENTATION

The parameters referred to in this report are listed below together with their symbols and instrumentation:

Temperature, Centigrade	t	Measured by ML-471/AMQ-8 indicating resistance thermometer. This instrument measures accurately to $\pm$ 0.5°C, and reproduces its indication at $\pm$ 0.1°C.
Temperature, Absolute	T	t$^{\circ}$C + 273.15°
Total pressure, atmospheric	p	Millibars. Obtained from B-29 altimeter.
Microwave refractive modulus	N	"N units." Measured by University of Texas type microwave refractometer installed in C-131.
Relative humidity	e/e_s	Computed from N, T, and p.
Path function	$B_*(z,\theta,\emptyset)$	Foot lamberts per nautical mile. Measured by attenuation meter mounted on B-29 fuselage. The parenthetical subscripts are: z - altitude in feet θ - zenith angle of line of sight $\emptyset$ - azimuth angle of line of sight and sun's bearing
	$_A B_*(z,\theta,\emptyset)$	For pure, dry air. Foot lamberts per nautical mile. Computed.
	$_P B_*(z,\theta,\emptyset)$	For particles in suspension. Foot lamberts per nautical mile. $_P B_* = B_* - {_A B_*}$

Volume Scattering Function $\sigma_\lambda(z; \emptyset')$ For unit length. This is
a function of altitude, z;
the angle between incident
and scattered flux, $\emptyset'$, and
wave length λ .

Volume attenuation function $\alpha(z)$ Per unit length. This is a
function of z(altitude). It
is the sum of s(z), the total
scattering function, and
a(z), the volume absorption
function.

Total scattering function   s(z)   Per unit length. This is a
function of altitude. It
equals the integral

$$\int_{4\pi} \sigma(z; \phi')d\Omega$$

DISCUSSION

Immediately after take-off from Patrick A.F. Base the B-29 and

C-131 climbed to altitude. During this ascent to station altitude

the ambient air temperature was recorded at one hundred feet inter-

vals and visual observations of the sky were recorded. The temperature

plot as a function of altitude is shown in Fig. 1. Added to the graph

are notes regarding observed clouds and haze layers. Overlaid on the

graph are solid lines which represent temperature lapse of saturated

air, often referred to as "wet adiabats."

Fig. 2 shows the temperature profile recorded during descent

from 18,000 feet to 8,000 feet, and from 8,000 feet to 500 ft. A

comparison of these two temperature profiles is of interest:

Differences Between Temperature Profiles for Ascent and Descent.

The ascent profile shows more fine structure than the descent profile.

This should not be given too much importance for the following reason:

The ascent was from 1336 to 1424, a time lapse of 48 minutes; the

descent from 1436 to 1457, and from 1501 to 1509, periods of 15 and

8 minutes respectively, or total of 23 minutes. Thus it is seen

that during the ascent the airplane covered at least twice the hori-

zontal distance than it did during descent. Now it is known that the

atmosphere is not homogeneous in that there are moisture cells present.

These cells are left after small cumulus clouds have evaporated, and

represent a greater concentration of water vapor than the air surrounding

them. They may be several hundreds of feet thick. Thus an airplane

climbing at a rate of approximately 300 ft/min at a forward speed of

150 knots or better, upon reaching a stratum of moisture cells might easily pass through several of these cells in succession while climbing through the stratum. (This is illustrated in Fig. 3). If there are temperature differences inside and outside of the cells the record would show the effect of each cell as the airplane continues its climb, and this might be interpreted as the airplane having gone through several temperature inversions. This is, of course, in error. Accordingly, the temperature recorded during descent is considered to be more representative of the true air temperature pattern.

During descent the temperature was recorded as being lower, generally, than during ascent. The descent started 12 minutes after arrival on station, it terminated 1 hour and 33 minutes after start of climb following take-off, the elapsed time being in mid-afternoon with the sun's zenith angle increasing toward the west. This would indicate that the temperature was in fact lowering. However, the shape of the descent profile at 18,000 ft. to 17,500 ft., i.e., a comparatively small change of temperature with altitude, may indicate a lag in altimeter readings. The fact that the inversion near 7,000 ft. is recorded approximately 200 ft. lower during descent might be interpreted as confirming an altimeter lag. However, because all data recorded during descent are correlated to that one parameter, the altimeter altitude, the effect of the error is minimal. Accordingly, the temperature recorded during descent has been used for all data reduction. Data recorded in the C-131 were synchronized with the B-29 data by voice radio.

Microwave Refractive Modulus. Fig. 4 is a plot of microwave refractive modulus as a function of altitude, and the corresponding relative humidity computed from microwave refractometer and other data. The microwave refractive modulus[4] is defined as follows:

$$N = (n-1) \ 10^6 \tag{1}$$

where n is refractive index of air. A typical value of the refractive index of air of 1.000300 is indicated as microwave refractive modulus of 300, often referred to as 300 "N units." The microwave refractometer measures N directly. Then by using the recorded centigrade temperature converted to absolute temperature and the atmospheric pressure corresponding to altimeter altitude, the partial pressure of water vapor, e , in millibars, is computed[4] from the following Debye equation:

$$N = \frac{77.6 \ p}{T} + \frac{77.6 \times 4810}{T^2} e \tag{2}$$

where N is in "N units," T is absolute temperature, and p is total atmospheric pressure in millibars.

Determination of Relative Humidity. By setting e = o , the second term of the right hand side of the above equation is zero, and $N = \frac{77.6 \ p}{T}$. This is the equation of microwave refractive modulus for dry air. This is plotted in Fig. 4, as the farthest to

the left. By setting $e = e_s$, the partial pressure of water vapor

at dew point temperature, the equation is

$$N = \frac{77.6\ p}{T} + \frac{77.6 \times 4810}{T^2} e_s$$

and the plot of this equation shows the microwave refractive modulus

for saturated air. The microwave refractive modulus for the ambient

air, if the air is not completely dry or saturated, must fall between

the two limiting curves. This it does.

Now the difference between the left limiting curve and recorded

N unit curve is $\dfrac{77.6 \times 4810}{T^2} e$, and the difference between the

two limiting curves is $\dfrac{77.6 \times 4810}{T^2} e_s$. Thus the ratio of these

two quantities is e/e_s, the approximate relative humidity.

Relative humidity is defined[8] as the ratio of observed and saturated

mixing ratios, the mixing ratios being:

$$\text{observed} - \frac{.622\ e}{p - e}$$

$$\text{saturated} - \frac{.622\ e_s}{p - e_s}$$

The ratio $\dfrac{.622\ e}{p - e} \bigg/ \dfrac{.622\ e_s}{p - e_s}$ reduces to $\dfrac{e}{e_s} \times \dfrac{p - e_s}{p - e}$,

but because e and e_s are very small compared to p, $\dfrac{p - e_s}{p - e} \doteq 1$

and relative humidity $\doteq e/e_s$.

Relative Humidity vs Altitude. The plot on the right side of Fig. 4 is relative humidity computed as a function of altitude. A comparison of the relative humidity with the observed clouds and haze layers indicated on Fig. 1, shows that the clouds at 3500-6000 feet correspond to high relative humidity, and the haze layer at 13000 feet corresponds to another stratum of increased humidity.

Path Function vs Altitude. Also recorded during descent was the path function, $B_*(z,\theta,\emptyset)$. (In this report the notation for path function $B_*(z,\theta,\emptyset)$ indicates the photopic case while $N_*(z,\theta,\emptyset)$, used in reference 4, indicates the general radiometric case.) The path function, a measure of the light flux being scattered from a volume of aerosol, is dependent on two things, the character of the illumination, and the character of the aerosol. If the geometry and intensity of the illumination remain constant, a change in the value of the path function indicates a change in the character of the aerosol.

During a change of altitude, if the character of the aerosol and geometry of lighting remain constant, there will be a regular change of path function due to the change in density of the aerosol, the path function at altitude being related to the path function at sea level by the equation

$$B_*(z, \theta, \emptyset) = B_*(o, \theta, \emptyset) \, e^{-z/k} \qquad (3)$$

where e is the natural logarithmic base, z is altitude in feet,

and k is the altitude in feet at which the path function at that

altitude is 1/e of path function at sea level. This altitude is

approximately 30,000 feet. This is one of the factors which characterizes

the "Optical Standard Atmosphere."[14]

In addition to the exponential change of B_* due to change of air

density there will be another change due to change in the character

of the aerosol. This is shown in Fig. 5. Plotted farthest to the

left is the $_AB_*(z,90°,90°)$ value as a function of altitude for pure

dry air. This was computed as follows:

Computation of Path Function for Dry Air. Tousey and Hulburt[15]

have defined the "optical scattering coefficient" by the equation

$$\lambda_{\phi\lambda} = \sigma_{\phi\lambda} \; \lambda_\lambda$$

In the notation used in this report the above equation is

$$_A N_{*\lambda}(z, \theta, \phi) = \sigma_\lambda(z; \phi') \times H_\lambda \tag{4}$$

where $_A N_{*\lambda}(z,\theta,\phi)$ is <u>radiance</u> value of electro-magnetic radiation

of wavelength λ being scattered at altitude z, zenith angle θ,

and solar azimuthal angle ϕ; $\sigma_\lambda(z; \phi')$ is the volume scattering

function for wavelength λ at altitude z, and angle between

incident flux and scattered flux of ϕ'; and H $_\lambda$ is the irradiance of

wavelength λ incident on the scattering volume. The volume

scattering function for the case of Rayleigh scattering is further

defined as[15]

$$\sigma_\lambda \left(0; \phi' \right) = \frac{2\pi^2}{N\lambda^4} \left(m-1 \right)^2 \left(1 + \cos^2\phi' \right) \tag{5}$$

where m is index of refraction of air; N is Loschmidt's number

2.687×10^{19}, the number of molecules per cm^3 of an ideal gas at

standard atmospheric pressure and $0^\circ C$; λ is wavelength; and ϕ'

is the scattering angles as defined above. Note that $\sigma_\lambda \left(0; \phi' \right)$

is now limited to an altitude of z = o, i.e., sea level. The $_AB_*$,

or <u>luminance</u> value of path function, the total scattered radiance

per cm^2 per steradian, at sea level, at zenith angle of 90°, and solar

azimuth angle of 90° (i.e. $\phi' = 90^\circ$), across the visible spectrum

was found by Eq (5) as follows:

$$_AA_* \left(0, 90^\circ, 90^\circ \right) = 680 \frac{2\pi^2}{N} \left(m-1 \right)^2 \sum_{400}^{700} S_\lambda T_\lambda \frac{H\lambda}{1000} \lambda^{-4} \Delta\lambda \times F$$

where 680 is the luminous efficiency term; $S_\lambda T_\lambda$, the

normalized product of spectral sensitivity of phototube and spectral

transmittance of filter (ideally this is equal to $\bar{y}$, the luminous

efficiency factor as a function of wavelength, but in this case $S_\lambda T_\lambda$

is the real value for the phototube-filter combination, being slightly

different than $\bar{y}$.); $H\lambda$ the solar irradiance outside the earth's

atmosphere in watts cm^{-2} u^{-1} as tabulated by Johnson[10]; λ is

wavelength in cm; $\Delta\lambda$ bandwidth of 10 mu; and F being conversion

units necessary to produce an answer in foot-lamberts per nautical

mile. The value was computed to be

$$_\Lambda B_*(0,90°,90°) = 12.97 \text{ Foot-lamberts/nautical mile.}$$

$_\Lambda B_*$ $(z,90°,90°)$ was determned for 20,000 feet altitude by Eq. 3.

$$_\Lambda B_*(20000,90°,90°) = {}_\Lambda B_*(0,90°,90°) \; e^{-\frac{20000}{30000}}$$

and, because Fig. 5 is a semi-logarithmic plot, $e^{-z/30,000}$ plots

as a straight line between the two end points $_\Lambda B_*(0,90°,90°) = 12.97$

foot lamberts/nautical mile and $_\Lambda B_*(20,000,90°,90°) = 6.67$ foot lamberts/

nautical mile.

Measured Path Function vs Altitude. Next was plotted the measured
$B_*(z,90°,90°)$. The difference between the measured B_* and the $_\Lambda B_*$
(computed for ~ure, dry air) is the effect of liquid water in suspension,
and to a lesser degree, industrial haze, smoke particles, or any other
material in suspension.

Relative Humidity vs Altitude. Also on Fig. 5 there is a plot of
relative humiditv. The only difference between the plots of relative
humidity in Figs. 4 and 5 is the choice of horizontal coordinates, being
linear in Fig. 4 and logarithmic in Fig. 5. The similarity between
path function and relative humidity profiles is easily seen.

Path Function Not Affected by Water Vapor. Now the path function

as measured does not indicate the presence of water vapor. Rayleigh

scattering is defined as the scattering from very small particles

including the molecules of air.[9] The atmosphere is made up of air, i.e.,

approximately 75.5% nitrogen, 23.15% oxygen, 1.28% argon, traces of

other gases, and water vapor and liquid water in varying amounts.[1] If

we postulate a dry atmosphere, i.e., one of nitrogen, oxygen, argon,

and traces of other gases, and to this we add water vapor, each water

vapor molecule must displace a gas molecule in order that the pressure

remain the same. Then any increases of scattering due to water vapor

can be computed as follows:

The total scattering function for Rayleigh scattering from gas

molecules given by Johnson[11] as "scattering coefficient" is

$$ \mathcal{A}(o) = \frac{32 \pi^3}{3 N \lambda^4} (m - 1)^2 \qquad (4)^* $$

where N is the number of scatterers, λ the wavelength of light, and

m the index of refraction of the gas.

The indices of refraction at standard atmospheric pressure and $0^{\circ}C$ of

N_2, O_2, and H_2O vapor are, respectively, 1.000249 to 1.000259, 1.000271,

and 1.000296 to 1.000298[6]. The maximum possible increase due to water

vapor would be when H_2O molecules displaced N_2 molecules and this increase

---

* Eq. 4 applies to gas at standard atmospheric pressure, i.e., at sea
level, hence s(z) = s(o).

would be

$$\frac{(m-1)^2_{H_2 O}}{(m-1)^2_{N_2}} = \frac{(1.000298 -1)^2}{(1.000249 -1)^2} = 1.43$$

or 43 percent. But at standard atmospheric pressure of 1013.25 mb. and temperature of 15°C, the water vapor pressure is 17 mb. or 1.6 percent of the total pressure. Because the partial pressures of a mixture of gases is proportional to the numbers of molecules of the gases in the mixture the H_2O molecules would be 1.6 percent of the total molecules in the gas. This means that if all of the water vapor molecules introduced into the gas displaced only nitrogen molecules, the increase of total scattering function due to the water vapor would be .43 X .016 = .00688, i.e., 0.7 of 1 percent. This precision cannot be achieved in the attenuation meter by which path function is measured.

Liquid Water Indicated by Measured Path Function. The path function does indicate the presence of liquid water or other scattering material in the atmosphere. The preceding paragraph dealt with molecular scattering only, i.e., pure, dry air. According to Fritz[7] the atmosphere is never pure nor dry, but dust and water vapor are always present in varying degrees. van de Hulst[16] states that the scattering coefficient for Rayleigh molecular scattering varies as a function of λ^{-4}, and the scattering coefficient has been found to increase with increasing humidity. He further states that this increase is larger than that caused by molecular scattering of water vapor and that some of the molecules form small droplets or clusters of molecules. Junge,[12] reporting Wall, makes the following distinction between different types of nuclei:

(1)   Particles insoluble in water and unwettable. These

may serve as nuclei of condensation, but to do so require

a large amount of super saturation. Their importance for

the natural aerosol is slight.

(2)   Particles insoluble in water, but wettable.

(3)   Droplets of solution.

From certain evidence Junge[12] states that it appears that in the atmos-

phere there is a preponderance of droplets of solution.

The particles in the air vary in size from 10^{-6} to 10^{-1} cm. The

size range from 10^{-6} to 10^{-1} cm covers two general classes of particles,

"small" and "large," i.e., those having diameters of 10^{-5} cm or smaller

which cause Rayleigh scattering, and those having diameters larger than

10^{-5} cm which cause Mie scattering. These particles, both "small"

and "large," cause increase in path function over that due to molecular

scattering only.

The total scattering function for Rayleigh scattering, i.e.,

small particles, but larger than molecules, is given by the following

equation:[11]

$$ A(0) = 24 \pi^3 N \left(\frac{n^2-1}{n^2+2} \right)^2 \frac{V^2}{\lambda^4} \tag{5} $$

where N is the number of scatterers, n is the index of refraction

of the scattering medium (for water, n = 1.33), V is the volume of

the scatterers, and λ is the wavelength of light. The total scattering

function for Mie scattering is given by the same equation modified

as follows:[11]

$$\mathscr{A}(0) = 24\pi^3 N \left(\frac{n^2-1}{n^2+2}\right)^2 \frac{V^2}{\lambda^4} \left[1 + \frac{6\pi^4}{5}\left(\frac{n^2-1}{n^2+2}\right)\frac{a^4}{\lambda^4}\cdots\right] \quad (6)$$

From these two equations it can be seen that the scattering coefficient varies directly as the number of scatterers, the square of the volumes of the scatterers, and, when the particles are "large," as the series enclosed in the brackets.

Molecular Scattering vs Particle Scattering. A comparison between the scattering coefficients for pure, dry air, i.e., molecular scattering, and for very small particle   Rayleigh scattering. follows:

(1) For molecular scattering, Eq. 4 is used, which may be rewritten as follows:

$$\mathscr{A}(0) = \frac{32}{3N}\left(m-1\right)^2 \frac{\pi^3}{\lambda^4}$$

Let m be a weighted average of the indices of refraction for 75 percent nitrogen and 25 oxygen equal to 1.000262; N is Loschmidt's number, 2.687×10^{19}, the number of molecules per cm^3 of an ideal gas at standard atmospheric pressure and $0^\circ C.$[13] Then, for molecular scattering, the total scattering function is

$$\mathscr{A}(0) = 2.73 \times 10^{-26} \frac{\pi^3}{\lambda^4}$$

(2) For Rayleigh scattering, Eq. 5 is used, and may be rewritten as follows:

$$\mathscr{A}(0) = 24 N \left(\frac{n^2-1}{n^2+2}\right)^2 V^2 \frac{\pi^3}{\lambda^4}$$

Let n be 1.33, the index of refraction of water; V, the volume of

one small particle having a radius of 10^{-6} cm, equal to 4/3 π X 10^{-18}

cm^3; and N = 1. Then, for Rayleigh scattering by one small particle,

the total scattering function is

$$\mathcal{A}(0) = 1.78 \times 10^{-35} \frac{\pi^3}{\lambda^4}$$

To compare the above total scattering function with the total scattering

function for molecular scattering, it is multiplied by 2.687 X 10^{19},

Loschmidt's number, so that there are the same number of scatterers

per unit volume, in this case, cm^3, then

$$\mathcal{A}(0) = 4.78 \times 10^{-16} \frac{\pi^3}{\lambda^4}$$

and the ratio of total scattering functions, particle to molecular, is

$$\frac{4.78 \times 10^{-16}}{2.73 \times 10^{-26}} \doteq 2 \times 10^{10}$$

Thus any small water particle that displaces an air molecule or is

added to a volume of pure, dry air will, under any circumstances,

increase the scattering. And, conversely, any increase in path function

over the value due to molecular scattering is due to particles which

are predominately liquid water. This discussion is not intended to

be construed as saying that liquid water and liquid water alone is

necessarily the sole cause of the scattering increase as indicated by a

path function measurement, for there is always the possibility that

non-hygroscopic particles may be present.

Microwave Refractive Modulus Independent of Liquid Water. The
microwave refractometer when properly calibrated measures the micro-
wave refractive modulus, N, directly. The microwave refractive modulus
is a function of three variables, viz., temperature, total atmospheric
pressure, and the partial pressure of water vapor present in the
atmosphere.[2] There is some disagreement concerning the effect of liquid
water on the operation of the microwave refractometer, but according to
Enenstein[5] there is some effect. Cunningham, Plank, and Campen[3] find
that the effect of liquid water, using Enenstein's equation is approxi-
mately 0.6N units for clouds, 0.5N units for rain, maximum, this is
less than 1 percent of a typical value of atmospheric microwave
refractive modulus. Inasmuch as the data presented in this paper were
recorded for clear, i.e., cloud free weather, the effect of liquid
water is negligible. Thus the relative humidity profile is valid.

Correlation Between Path Function and Relative Humidity. Correla-
tion between the path function and relative humidity profiles was
made by the following steps:

(1)   The difference between the measured path function and the
       path function for pure, dry air, i.e., the effect of liquid
       water and other materials in suspension, was tabulated
       for each 100 feet. This is $_pB_*(0,90^\circ,90^\circ)$

(2)   The above differences were normalized at the maximum value.

(3)   The normalized path function $_pB_*$ values were plotted
       vertically against the relative humidity values plotted
       horizontally. This is Fig. 6.

RESULTS

In general Fig. 6 shows that with high relative humidity values,
above 80 percent, small changes of relative humidity are accompanied
by large changes in path function; that with low relative humidity
values, below 60 percent, large changes of relative humidity are
accompanied by small changes cf path function; and from 65 percent
relative humidity to 85 percent relative humidity another relationship
exists.

Discussion . Middleton[15] states that there is comparatively
little change in the radii of liquid droplets with changes of relative
humidity below about 70 percent, and Fig. 6 tends to bear this out.
The plot of relative humidity values from 67 percent to 85 percent
and $_pB_*$ values of .22 and .35 seem to be anomalous in that it forms
a reverse curve.

The data plotted in Fig. 6 were recorded in two airplanes flying
several hundreds of feet apart, with the refractometer equipped airplane
flying slightly behind and higher than the B-29. Thus it would appear
that the data might be affected by the airplane flying through inhomo-
geneous aerosol, i.e., through different moisture cells. The effect
from this would more than likely be of a random nature, while the
plot of the reverse curve in Fig. 6 does not show randomness.

All of the data plotted in Fig. 6 were recorded while flying over
the Atlantic Ocean in the vicinity of Patrick Air Force Base. It is
of interest that the data in question, i.e., the reverse curve plot,

were the data recorded from 2000 feet altitude down to 1000 feet

altitude. Woodcock and Gifford as reported by Junge[12] deposited

haze droplets on small glass plates and showed that over the ocean

practically all these droplets consists of NaCl solutions. And Simp-

son and Wall, again as reported by Junge[12], have pointed out that in

the case of crystallization of NaCl from droplets the size of droplets

is bound to decrease in a discontinuous manner until all water is

evaporated. It is possible that some such process is responsible for

the apparent discontinuity in Fig. 6.

Recently a microwave refractometer was installed in the Visibility

Laboratory equipped B-29 with its probe located within two feet of

the attenuation meter by which path function is measured. It is expected

that data from future flights will show less deviation than that

reported herein, and it is expected that it can be determined whether

the reverse curve is a real effect or not.

ACKNOWLEDGEMENTS

REFERENCES

1. Berry, F. A. Jr., E. Bollay, and N. R. Beers, Handbook of Meteorology, McGraw-Hill, New York, pp. 351 and 373, (1945).

2. Crain, C. M., and J. R. Gerhardt, "Some Preliminary Studies of the Rapid Variations in the Index of Refraction of Atmospheric Air at Microwave Frequencies," Bulletin of the American Meteorological Society, 31, pp. 330-331 (1950).

3. Cunningham, R. M., V. G. Plank, and C. F. Campen, Jr., "Cloud Refractive Index Studies," Geophysical Research Papers, No. 51, Air Force Cambridge Research Center, p. 2, (1956).

4. Duntley, S. Q., A. R. Boileau, and R. W. Preisendorfer, "Image Transmission by the Troposphere I, "Journal of the Optical Society of America, 47, pp. 499-506, (1957).

5. Enenstein, N. H., "The Effect of Water Droplets on the Index of Refraction," Proceedings, Symposium on Tropospheric Wave Propogation, U. S. Navy Electronics Laboratory Report No. 173, p. 52, (1948).

6. Eshbach, O. W., Handbook of Engineering Fundamentals, John Wiley and Sons, New York, P. 9-15. (1949).

7. Fritz, Sigmund, "Solar Radiant Energy and its Modifications by the Earth and its Atmosphere," Compendium of Meteorology, American Meteorological Society, Boston, p. 23, (1951).

8. Haltiner, G. J., and Frank L. Martin, _Dynamical and Physical Meteorology_. McGraw-Hill, New York, pp. 23-24, (1957).

9. _International Dictionary of Physics and Electronics_, Walter C. Michels, Senior Editor, Van Nostrand Co., New York, p. 804, (1956).

10. Johnson, Francis S., "The Solar Constant," _Journal of Meteorology_, 11, pp. 431-439, (1954).

11. Johnson, John C., _Physical Meteorology_, M.I.T. Tech. Press and John Wiley and Sons, New York, pp. 33-44, (1954).

12. Junge, C., "Nuclei of Atmospheric Condensation," _Compendium of Meteorology_, American Meteorological Society, Boston, p. 188, (1951).

13. Middleton, W.E.K., _Vision Through the Atmosphere_, Univ. of Toronto Press, Toronto, pp. 20-24 (1952).

14. Preisendorfer, R. W., _Theory of Attenuation Measurements in Planetary Atmospheres_, SIO Ref. 58-81. Scripps Institution of Oceanography, University of California, La Jolla, Calif., 24 Nov 1958.

15. Tousey, R., and E. O. Hulburt, "Brightness and Polarization of the Daylight Sky at Various Altitudes above Sea Level," _Journal of the Optical Society of America_, 37, pp. 78-92, (1947).

16. Van de Hulst, H. C. _The Atmosphere of Earth and Planets_, edited by C. P. Kuiper, Univ. of Chicago Press, Chicago, pp. 55-56 (1948).
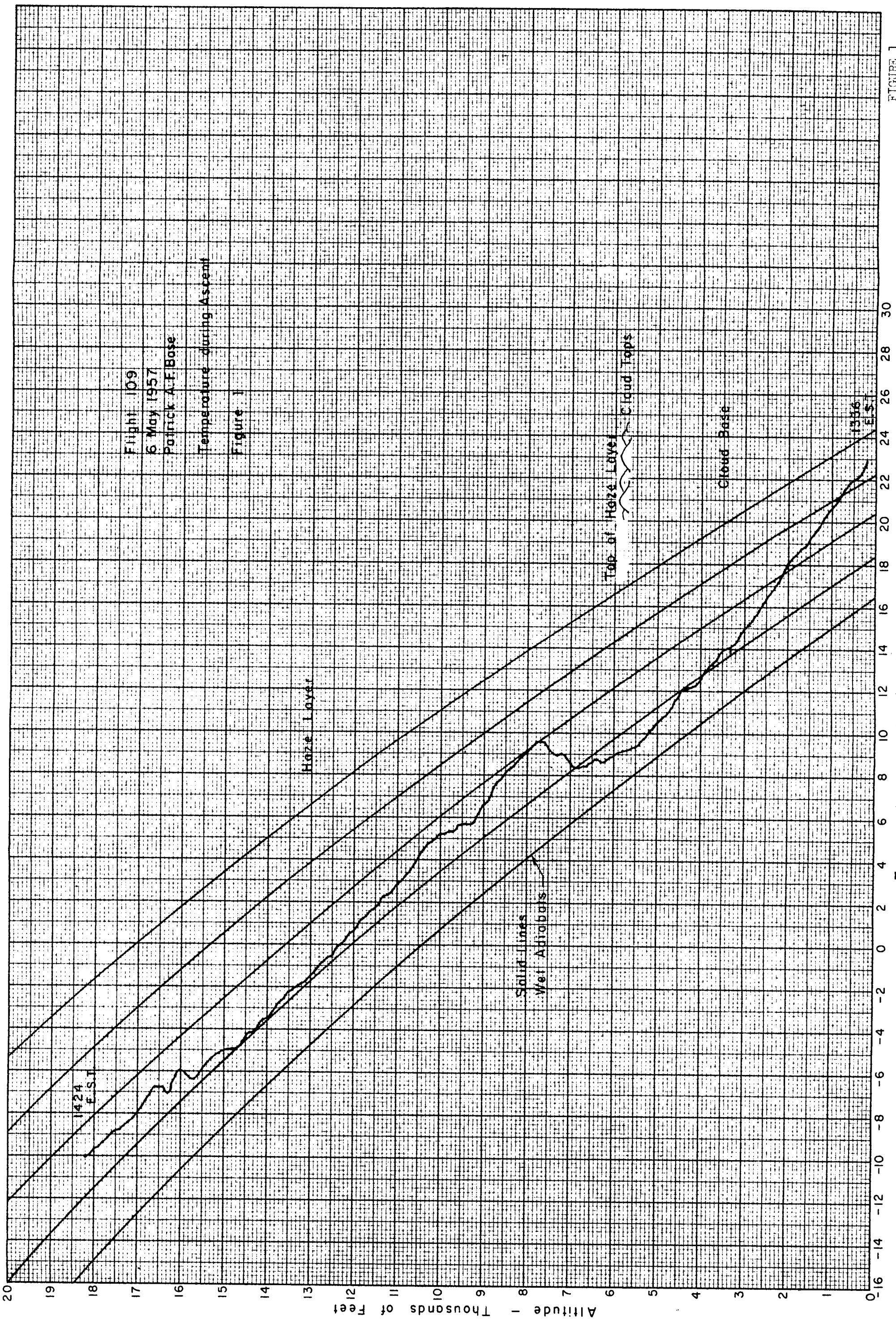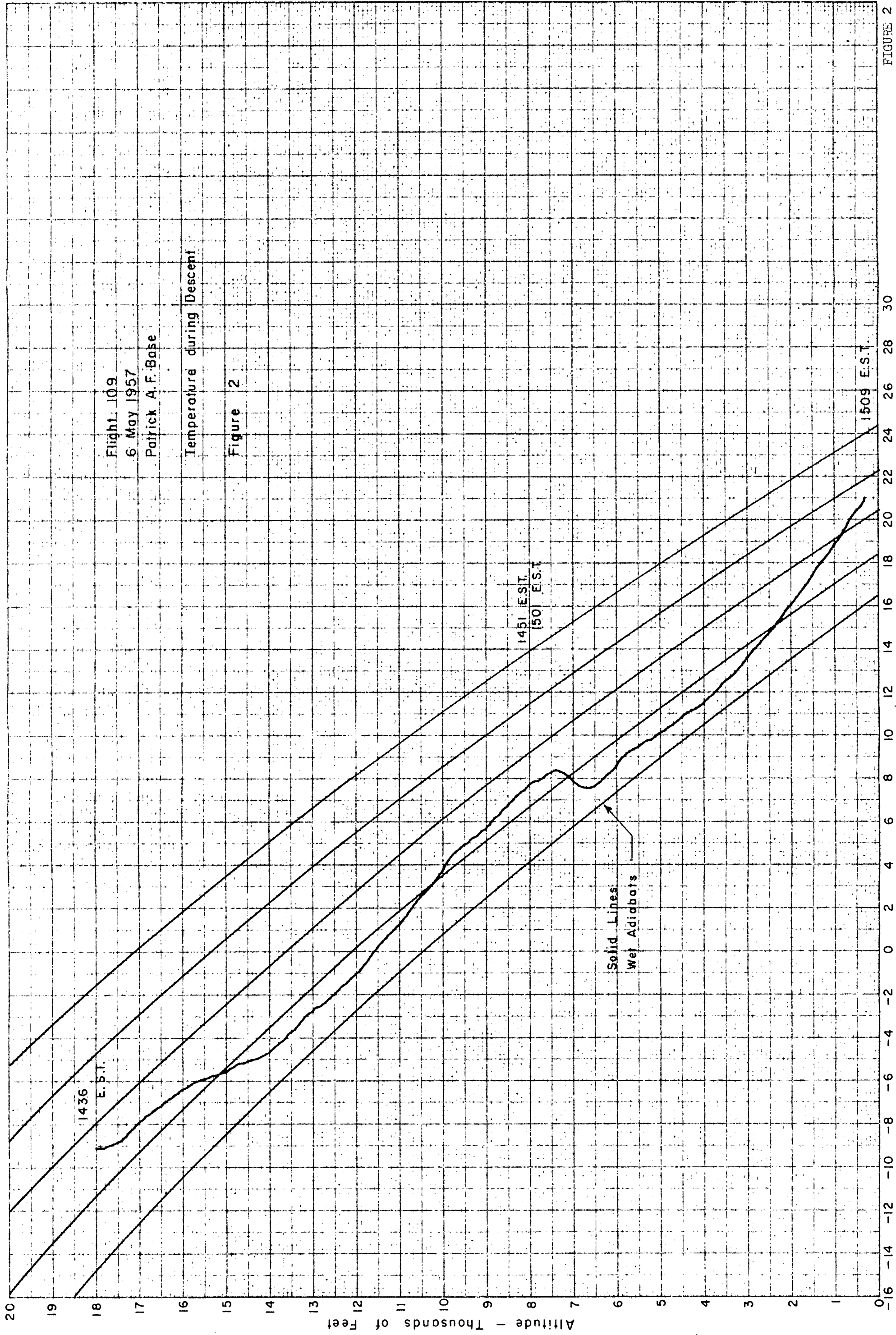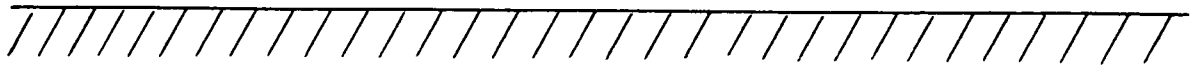
ARB:deg
1/10/59

Figure 1

Flight 109
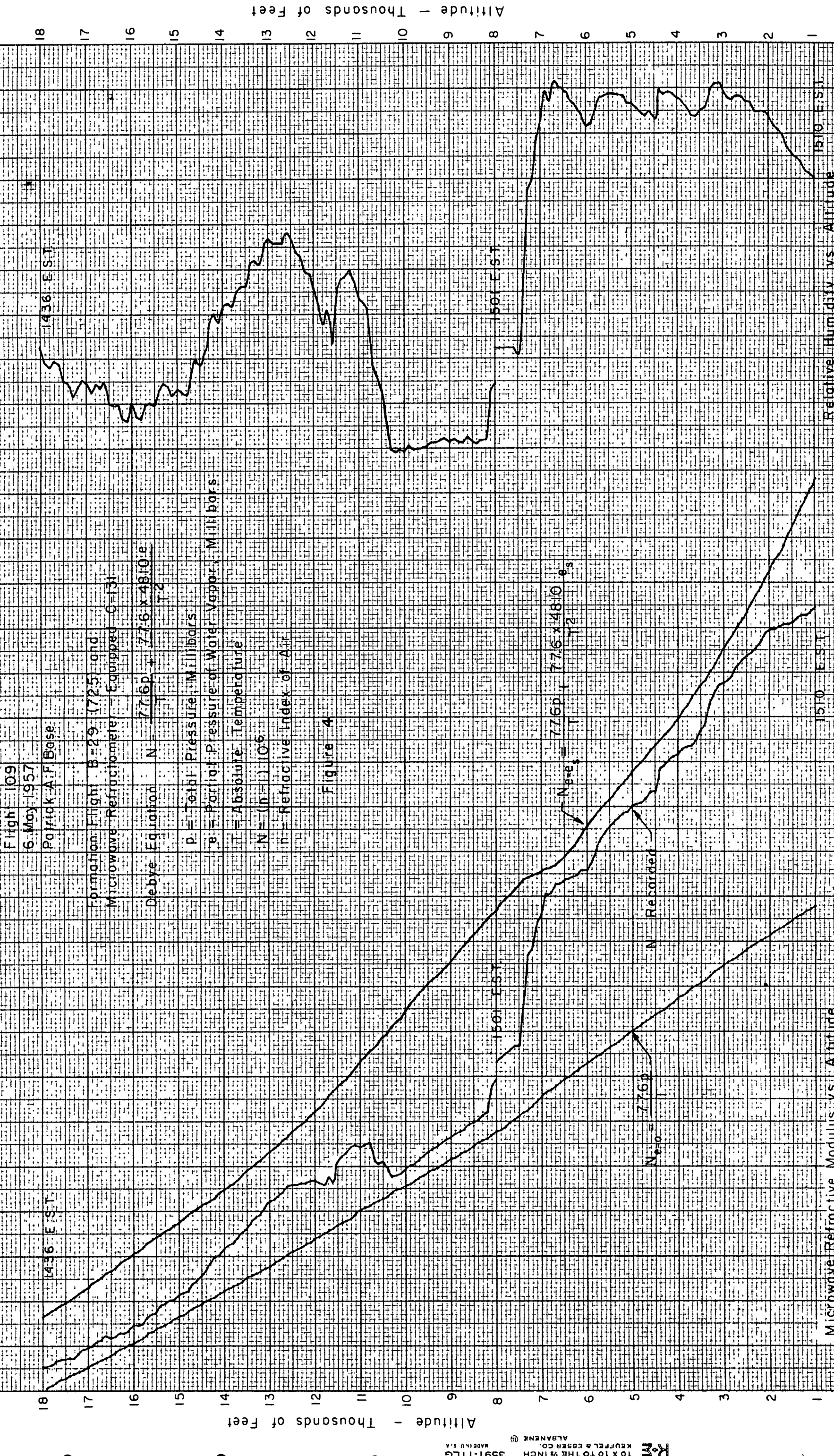6 May 1957
Patrick A.F. Base

Temperature during Ascent

Figure 1

Haze Layer

Top of Haze Layer — Cloud Tops

Cloud Base

1306 E.S.

1424 F.S.

Solid lines
Wet Adiabats

Altitude — Thousands of Feet

Temperature — Centigrade — (Vortex Thermometer)

FIGURE 2

Flight 109
6 May 1957
Patrick A.F. Base

Temperature during Descent

Figure 2

1451 E.S.T.
1450 E.S.T.

1436 E.S.T.

1509 E.S.T.

Solid Lines
Wet Adiabats

Altitude — Thousands of Feet

Temperature — Centigrade — (Vortex Thermometer)

Stratum of Moisture Cells

Sea Level

Figure 3

Figure 4

ALTITUDE – THOUSANDS OF FEET

RELATIVE HUMIDITY e/e_s'

1436 E.S.T.

1451 E.S.T.
1501 E.S.T.

1510 E.S.T.
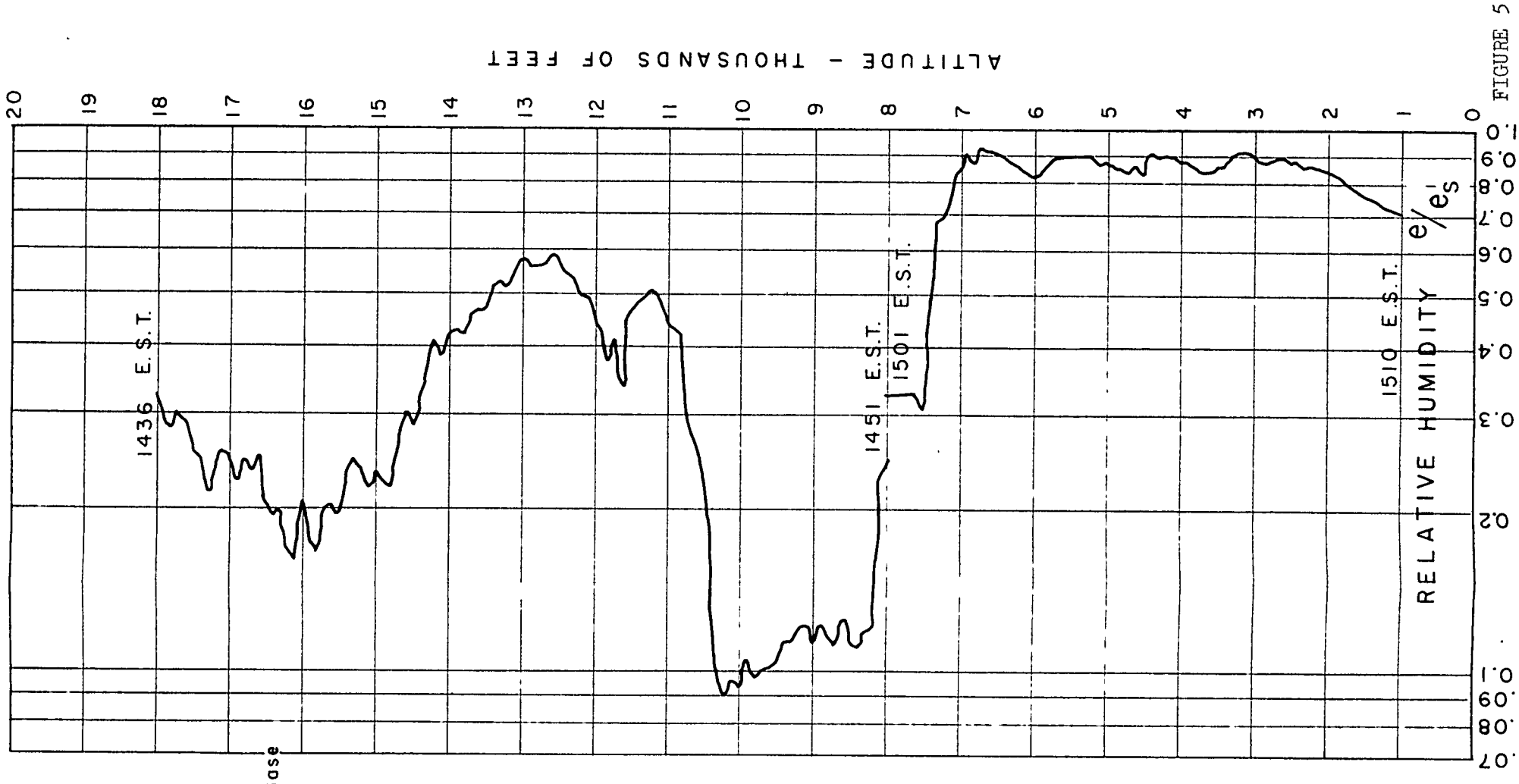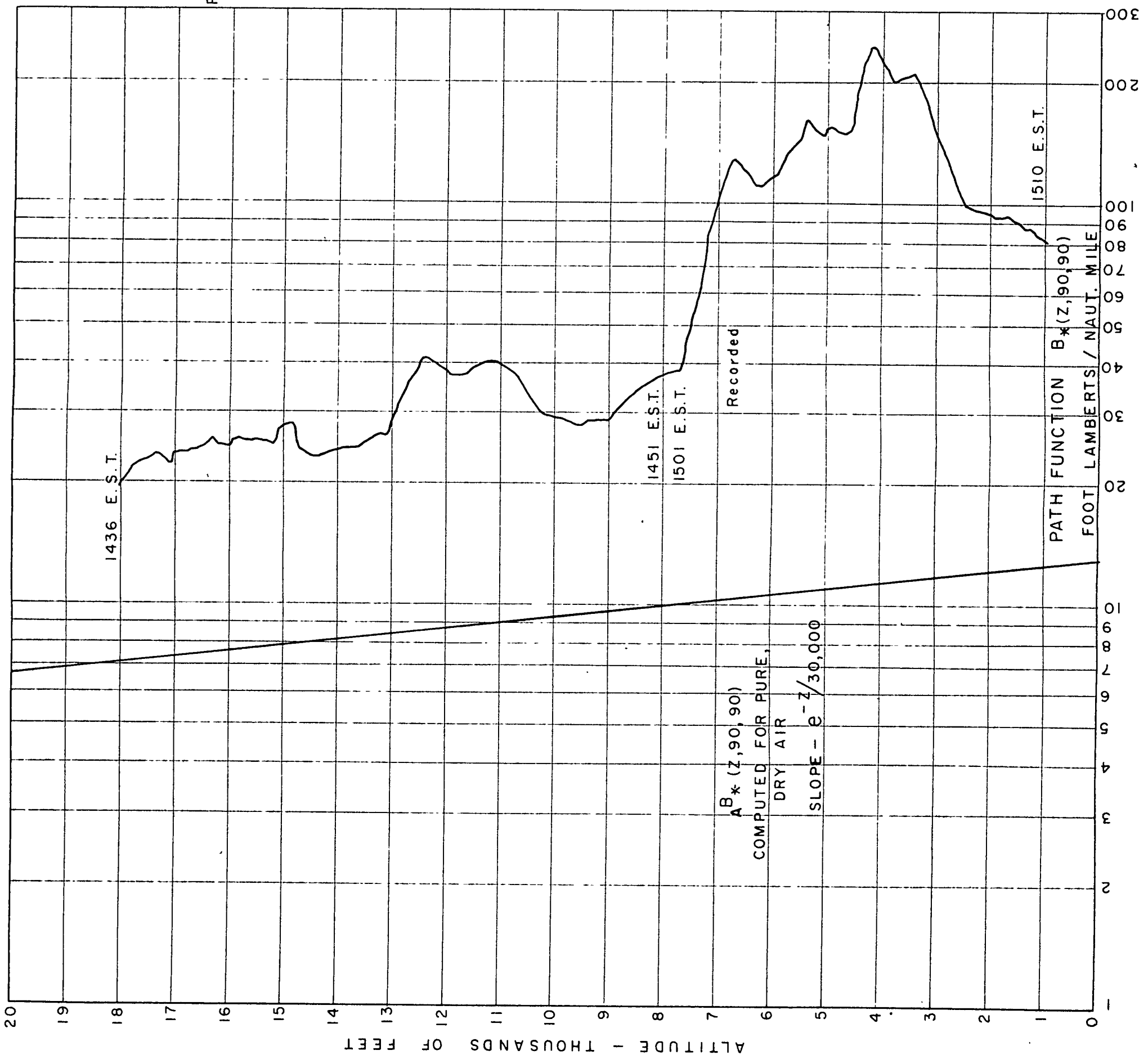
Flight 109
6 May 1957
Patrick A.F. Base

Figure 5

PATH FUNCTION $B_*(z,90,90)$
FOOT LAMBERTS / NAUT. MILE

$A^B_*(z,90,90)$
COMPUTED FOR PURE,
DRY AIR
SLOPE – $e^{-z/30,000}$

Recorded

1436 E.S.T.

1451 E.S.T.
1501 E.S.T.

1510 E.S.T.

ALTITUDE – THOUSANDS OF FEET

FIGURE 5